PHYSICAL REVIEW B VOLUME 20, NUMBER 10 15 NOVEMBER 1979

Study of the phase diagrams of the two-component electron-hole liquid in stressed germanium

G. Kirczenow*
Department of Physics and Astronomy, Northwestern University, Evanston, Illinois 60201

K. S. Singwi
Department of Physics and Astronomy, Northwestern University, Evanston, Illinois 60201
and Argonne National Laboratory, Argonne, Illinois 60439
(Received 24 May 1979)

We present a theoretical study of the phase equilibria of the electron-hole drop (EHD) containing two inequivalent electron species ("hot" and "cold" electrons) in ⟨111⟩-stressed Ge. We assume that transitions between the hot and cold electron states can be ignored and that the exchange-correlation energy density of the EHD depends only on the total density of the two electron species. We predict that for intermediate values of the stress at $T=0$ the EHD separates into two phases if the concentration of hot electrons in the EHD is not too high. One phase consists entirely of cold electrons and holes while the other phase contains both hot and cold electrons. We also discuss the phase diagrams of this system at finite temperatures. A variety of phase diagrams is predicted, different ones for different stress values. If our predictions are verified experimentally the two-component EHD would be a unique laboratory system whose closest analog is the fluid of neutrons and protons in neutrons stars.

I. INTRODUCTION

The electron-hole drop (EHD) phenomenon in highly excited semiconductors has during recent years received a great deal of attention both theoretically and experimentally.[1] The EHD is a Fermi liquid consisting of electrons and holes. Until recently, in all known cases its thermodynamic behavior was that of a one-component system because of the charge neutrality constraint that the numbers of electrons and holes should be equal. Recent experiments[2-4] have shown that in the case of the EHD in a Ge crystal which has been stressed along the ⟨111⟩ axis it is possible for there to be present two inequivalent types of electron so that the EHD then becomes effectively a two-component system. The ⟨111⟩ uniaxial stress raises the energy of three of the conduction valleys of the Ge crystal while lowering that of the fourth valley. Because of the large change in crystal momentum involved in transferring an electron from one valley to another in Ge, EHD electrons can remain trapped for times ~1 μsec in the three upper valleys before decaying into the lower valley.[2] This is a sufficient time for the electrons in the upper valleys (which we will refer to as "hot" electrons) to thermalize within the upper valleys, although their Fermi level need not be the same as that of the "cold" electrons in the lower valley. If one ignores the slow transfer of electrons between valleys, one can treat the hot and cold electrons as two separate species in quasiequilibrium with each other and with the holes. This approach will be adopted in the present paper. The nature of our idealization is similar to that which has been widely made in EHD calculations when only one electron species is present. That idealization has been to ignore the decay of the conduction electrons into the valence band and thus to treat the electrons and holes as two distinct species in equilibrium with each other.[5-8] We expect our present assumption to be equally realistic because the measured electron intervalley scattering time[2,4] in pure crystals is comparable with (although shorter than) the time it takes for an EHD electron to decay into the valence band, i.e., if the intravalley electron thermalization time is much shorter than the time which it takes for an electron to decay into the valence band, then it should also be much shorter than the intervalley scattering time.

By varying the experimental conditions it is possible to vary the relative numbers of "hot" and "cold" electrons in the EHD.[4] Thus, the EHD in stressed many-valley semiconductors provides a unique opportunity to study the thermodynamics of a degenerate two-component Coulomb Fermi liquid.

While the two-component quantum fluid ^{3}He-^{4}He has been studied extensively in the laboratory and its phase diagram is phenomenologically understood,[9,10] the only two-component degenerate Fermi system which has been studied in detail even theoretically has been the fluid of neutrons and protons in neutron stars.[11] At $T=0$ this system is believed to contain nuclei in a sea of neutrons, and at higher temperatures to consist of one or two phases with different neutron-proton density ratios.[12] The details of its phase diagram are important to the theory of stellar collapse.[13]

The EHD is a somewhat simpler system theoretically because the Coulomb interaction is not only known exactly but is simpler than the nuclear forces, and because in the case of the EHD we do not need to consider surface effects since all of the phases are macroscopic. The main difficulty is in estimating the exchange-correlation energy. This is complicated by the involved band structure of stressed Ge. However, the details of the band structure do not influence strongly the exchange-correlation energy of the EHD. The exchange-correlation energy appears to have a strong dependence only on the total density of electrons in the system and not, for instance, on the way in which the electrons are distributed among the different valleys. (In the cases in which such "band structure" effects have been evaluated numerically, it has been found that the exchange and correlation energies can each depend quite strongly on the number of valleys occupied by electrons, and on the degree of band anisotropy, but that their sum does not.[14,15] Thus, we choose to approximate the exchange-correlation energy of the EHD in stressed Ge by the exchange-correlation energy of the EHD for a model system with a simpler band structure, i.e., we approximate the exchange-correlation energy of the EHD for a given total density n of hot and cold electrons (irrespective of how the electrons are distributed among the different valleys) by the exchange-correlation energy of the EHD for the model system at the same density n. We will discuss two different model band structures:

(i) A "zero stress" model band structure with four equivalent spherically symmetrical conduction valleys and two decoupled spherical valence bands of equal mass equally populated with electrons and holes, respectively. This is model I in the notation of Bhattacharyya *et al.*[8] and we use the numerical correlation energies which they label SPH (self-consistent particle-hole approximation). We denote this choice of exchange-correlation energy E_{xc}^{0}.

(ii) A model band structure which corresponds to the limiting Ge band structure at large $\langle 111 \rangle$ stress, i.e., only one ellipsoidal conduction band and one ellipoidal valence band are populated. For this model we use the numerical correlation energy listed by Vashishta *et al.*[7] as "Ge $\langle 111 \rangle$ fully self-consistent anisotropic." We denote this model exchange-correlation energy by E_{xc}^{∞}.

It is important to use with each of the above correlation energies the exchange energy which corresponds to exactly the same model band structure for which the correlation energy was calculated, i.e., exactly those band structure features which are included in the correlation energy calculation should be included in the exchange. This point has been discussed in Ref. 14 and we shall discuss it further in the final section of this paper.

The hole kinetic energy is calculated in the Pikus and Bir[16] $\vec{k} \cdot \vec{p}$ formalism using the valence band parameters measured by Hensel and Suzuki.[17] Such a detailed treatment of the hole kinetic energy is essential. This is because the effect of the stress-induced splitting and associated nonparabolicity of the valence band on the hole kinetic energy has a decisive role in determining the nature of the phase diagrams of this system. Full account is taken of the distribution of electrons among the hot and cold valleys in calculating the electron kinetic energy.

A brief account of some of our results has already been published.[14,18] Our calculations predict that this EHD system has some interesting similarities with the above astrophysical one. At certain values of the stress, at $T=0$, if the concentration of hot electrons in the EHD is low enough, we predict that the EHD should separate into two phases, one consisting of cold electrons (and holes) while the other contains both hot and cold electrons. Thus, the hot and cold electrons in the EHD have a role analogous to that of the protons and neutrons respectively in the neutron star. This phase separation at $T=0$ was found for both of the model exchange-correlation energies described above and also for all other model exchange-correlation energies which we examined.

From the point of view of experimental verification of this predicted phase separation it is very important to have some idea as to how the system should behave for $T>0$. We studied this problem for three different values of the stress using the exchange correlation energy E_{xc}^{0} and a generalization of the method first used by Combescot[19] to calculate the EHD critical point in the one-component case. That method has been found to work very well at zero stress.[1] It has also been used with good results for stressed Ge in the case where only one conduction valley and one valence band are populated.[20] The numerical values E_{xc}^{0} of the exchange-correlation energy were chosen for this calculation because this choice results in very good agreement with available experimental data in the limiting case (which we call the "equilibrium limit") where the hot electrons have relaxed by intervalley scattering to the point where either the hot and cold electron Fermi levels have become equal or no electrons remain in the upper valleys.[15,21,22]

We find that in the $T>0$ range under suitable conditions it is possible to have two liquid phases in equilibrium with each other and with the vapor phase. The two liquid phases both contain hot and

cold electrons and holes. They differ from each other in that they have different ratios of hot to cold electrons and different total electron number densities. The vapor phase also consists of hot and cold electrons and holes (which may or may not combine into excitons and other complexes). Our main aim was to determine under which conditions the simultaneous presence of the two liquid phases and vapor is possible since this is the information of greatest experimental interest. This information is contained in the coexistence curves for three-phase equilibrium. These curves give the total density $n=n_h+n_c$ of hot and cold electrons and the concentration $x=n_h/n_c$ of hot electrons as a function of temperature in each of the three phases when all three phases are present in the system. We denote the densities of hot and cold electrons by n_h and n_c respectively. (At any fixed temperature, if all three phases are present, the value of n and of x in each phase is uniquely determined according to the Gibbs phase rule

$$f=C-P+2\,.$$

Here the number of components C is 2, the number of phases P equals 3 and thus $f=1$. This one available degree of freedom is taken up by specifying the temperature.)

Our calculations yield qualitatively different coexistence curves for each of the three values of stress studied. This implies that a remarkable variety of phase diagrams is possible in this system.

A particularly interesting case was found at low stress. There the two different liquid phases are found to coexist with each other and with the vapor in two different temperature ranges which are separated by a region where only one liquid phase is possible. To check how sensitive this phenomenon is to the choice of the exchange-correlation energy, we repeated the calculation at low stress using the exchange-correlation energy corresponding to the model band structure (i) above but taking the numerical correlation energy values which correspond to the Hubbard approximation[8] instead of the SPH. We denote this exchange-correlation energy E_{xc} (Hubbard). (The Hubbard and SPH correlation energies differ by about 10%.) The reappearance of the phase separation of the electron-hole liquid in a higher temperature range was found in this case as well.

II. THERMODYNAMICS

To study the phase equilibria of the EHD composed of hot electrons, cold electrons, and holes we need to know the hot and cold pair chemical potentials μ_h and μ_c and the pressure p which are defined in terms of the free energy $F(N_h, N_c, N_H, V, T)$ by

$$\mu_h=\left(\frac{\partial F}{\partial N_h}\right)_{N_c,V,T\ (N_H=N_c+N_h)}\,, \tag{1}$$

$$\mu_c=\left(\frac{\partial F}{\partial N_c}\right)_{N_h,V,T\ (N_H=N_c+N_h)}\,, \tag{2}$$

$$p=-\left(\frac{\partial F}{\partial V}\right)_{N_h,N_c,N_H,T}\,, \tag{3}$$

where N_H, N_h, N_c, and V are the numbers of holes, hot electrons, cold electrons, and the volume respectively. The derivatives of F are taken varying the number of holes together with the number of electrons in such a way that the electron-hole liquid is kept neutral, i.e., $N_h+N_c=N_H$ and $\delta N_h+\delta N_c=\delta N_H$. With this convention we will (except where there is danger of confusion) suppress N_H and write $F(N_h, N_c, V, T)$. Then the standard thermodynamic results for a two-component system will apply.

If S is the entropy, the equality

$$SdT-Vdp+N_h d\mu_h+N_c d\mu_c=0\,, \tag{4}$$

which holds for a two-component system, provides a simple way of determining whether a phase separation is possible for given values of p and T. From (4) the relation[23]

$$n_h d\mu_h+n_c d\mu_c=0 \tag{5}$$

holds on a thermodynamic surface of constant p and T, where $n=N/V$. Writing $x=N_h/N_c$ and integrating (5) at constant p and T yields

$$\mu_c(2)-\mu_c(1)=-\int_1^2 x d\mu_h\,, \tag{6}$$

i.e., if one plots μ_h versus x at constant p and T a Maxwell construction immediately shows whether or not two phases can exist in equilibrium. If μ_h versus x is monotonic increasing then there is no phase separation. In Fig. 1 in case (a) if $x_c'<x=N_h/N_c<x_c''$ (where x_c' and x_c'' are chosen so that the two shaded areas are equal) a separation occurs into two phases, one with $x=x_c'$ the other with $x=x_c''$. Case (b) represents a situation which we find to be characteristic of $T=0$ in an intermediate stress range. If $x>x_c$ (where x_c is given by the equal-area construction) the EHD is uniform and there is no phase separation. If $x<x_c$ a separation occurs into two phases: I where $x=0$ and II where $x=x_c$. Equation (6) guarantees that $\mu_c(\mathrm{II})=\mu_c(\mathrm{I})$, although $\mu_h(\mathrm{I})>\mu_h(\mathrm{II})$. This inequality is consistent with phase equilibrium since phase I ($x=0$) contains no hot electrons.

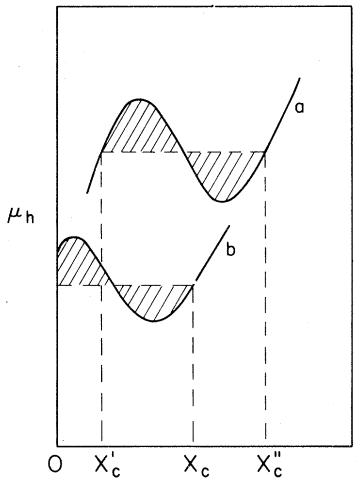

FIG. 1. Schematic plots of μ_h versus x at constant temperature and pressure.

The result (5) is *exact* and it should be possible to deduce all of the quantities n_h, n_c, μ_h, μ_c which it contains from the experimental EHD recombination spectra. For example, if the time evolution of the EHD created by a laser pulse is followed, the ratio $x=N_h/N_c$ will decrease with time because of the decay of the hot electrons into the cold valley. This means that μ_h and μ_c will change with time. Then, assuming that there is only one phase present and T and p are time independent, the incremental changes of μ_h and μ_c with time should obey Eq. (5). At sufficiently low temperatures, in such a time-resolved experiment, p will be very nearly time independent since it is equal to the pressure of the exciton vapor surrounding the EHD and, thus, always nearly equal to zero.

III. CALCULATIONS AND RESULTS AT $T=0$

Whether or not a phase separation of the two-component electron-hole liquid occurs under given conditions is a delicate question.

For example, it can be shown that within the Hartree-Fock approximation (HFA) at $T=0$ a phase separation of the liquid *always* occurs in two limiting cases, viz., when N_h/N_c is either very large or very small. However (as explained in the Appendix), the special feature of the HFA energy which results in the phase separation in these two limiting cases does not persist when correlations are properly included. Thus, a more careful treatment such as the one which we present in this paper is necessary in order to address meaningfully the question whether the phase separation should in fact occur. The fact that the model exchange-correlation energy densities which we use in our calculations depend only on the total density of electrons (as discussed in Sec. I) ensures the correct $n_h^{2/3}$ ($n_c^{2/3}$) dependence of μ_h (μ_c) on n_h (n_c) in the limit of small n_h (n_c) (see the Appendix). In this way we avoid the qualitative errors made by the HFA in these limiting cases. We still find that under certain conditions the EHD should phase separate. However, in contrast with the HFA results, our choice of exchange-correlation energy does not result in a phase separation in the limit of large N_h/N_c. Also, for small and moderate values of N_h/N_c we find that the phase separation is expected only in a certain range of stress values. As will be explained below, the situations in which we predict the phase separation to occur are those in which it is particularly favored by kinetic energy considerations.

At $T=0$, the free energy of the EHD equals

$$E=E_{\rm kin}^h+E_{\rm kin}^c+E_{\rm kin}^H+E_{xc}, \tag{7}$$

where $E_{\rm kin}^h$, $E_{\rm kin}^c$, $E_{\rm kin}^H$, and E_{xc} are, respectively, the kinetic energy of the hot electrons, cold electrons, and of the holes and the exchange-correlation energy. Define $N=N_h+N_c$ and $n=N/V$ to be the total electron number and number density of the EHD. Then if E_{xc}/N is taken to be a function only of the total density n, it follows that

$$\begin{aligned}\mu_h&=\mu_h^0+\mu_H^0+\mu_{xc},\\ \mu_c&=\mu_c^0+\mu_H^0+\mu_{xc},\\ p&=p_h^0+p_c^0+p_H^0+p_{xc},\end{aligned} \tag{8}$$

where

$$\mu_i^0=\left(\frac{\partial E_{\rm kin}^i}{\partial N_i}\right)_V, \quad p_i^0=-\left(\frac{\partial E_{\rm kin}^i}{\partial V}\right)_{N_i} \tag{9}$$

for $i=h$, c, or H

and

$$\mu_{xc}=\left(\frac{\partial E_{xc}}{\partial N}\right)_V, \quad p_{xc}=-\left(\frac{\partial E_{xc}}{\partial V}\right)_N. \tag{10}$$

To calculate μ_H^0 and p_H^0 we use the results of Ref. 15 which relate the hole density $n_H=n$ and hole kinetic energy $\epsilon^H=E_{\rm kin}^H/N_H$ to the hole Fermi energy $E_F(H)$ in $\langle 111\rangle$-stressed Ge. The relations between these quantities [as given by Eqs. (16)–(18) of Ref. 15] are

$$\epsilon^H=E_F(H)f_\epsilon(R), \tag{11}$$

$$n=[E_F(H)]^{3/2}f_n(R), \tag{12}$$

where

$$R=E_F(H)/S_H \tag{13}$$

and S_H is the magnitude of the stress-induced valence band splitting at the center of the Brillouin zone. The functions f_ϵ and f_n are evaluated numerically for the nonparabolic stress-split valence

band within the Pikus and Bir $\vec{k}\cdot\vec{p}$ formalism[16] using the valence band parameters of Hensel and Suzuki[17] as described in Ref. 15. We numerically invert (12) to obtain $E_F(H)$ and thus, via (11), ϵ^H as a function of n. Then using

$$\mu_H^0 = E_F(H) \tag{14}$$

and

$$p_H^0 = n(\mu_H^0 - \epsilon^H), \tag{15}$$

we obtain μ_H^0 and p_H^0 as a function of n.

For the electron kinetic energies we have

$$\epsilon^h \equiv E_{\rm kin}^h/N_h = \frac{3}{10}\frac{\hbar^2}{m_d}(\pi^2 n_h)^{2/3}, \tag{16}$$

$$\epsilon^c \equiv E_{\rm kin}^c/N_c = \frac{3}{10}\frac{\hbar^2}{m_d}(3\pi^2 n_c)^{2/3}, \tag{17}$$

where $m_d = (m_l m_t^2)^{1/3}$, $m_t = 0.082$, $m_l = 1.58$. Then

$$\mu_e^0 = \tfrac{5}{3}\epsilon^e \tag{18}$$

and

$$p_e^0 = \tfrac{2}{3} n_e \epsilon^e, \tag{19}$$

where e stands for h or c and μ_e^0 is measured from the bottom of the respective stressed conduction band.

In order to obtain p_{xc} and μ_{xc} it is necessary to interpolate and differentiate the correlation energy numerically. To do this, the published correlation energies[7,8] were smoothed and then interpolated by a cubic spline method. The derivatives were obtained from the spline coefficients. The main source of numerical error in our calculation is the limited accuracy to which the correlation energies are known. The exchange energies, which are also needed in order to obtain μ_{xc} and p_{xc} from (10), were calculated in the standard way[1] for the two model band structures described in Sec. I.

As noted in Sec. II, in order to determine whether a phase separation of the EHD should occur it is convenient to plot μ_h and μ_c versus $x = n_h/n_c$ at constant temperature and pressure. We calculate μ_h and μ_c making the "naive assumption" of a homogeneous EHD. We then infer from the results of this calculation the conditions under which the phase separation should occur and the properties of the phases. At $T = 0$ the vapor phase which is in contact with the EHD is the vacuum (since no excitons are present). Thus we are interested in the case $p = 0$.

For a fixed value of x we found numerically the value of the total density, n for which $p = 0$. Then for this value of n and x we calculated μ_h and μ_c. This procedure was repeated for different values of x. The resulting $p = 0$ isobars of μ_h, μ_c, n_h, and n_c for the model exchange-correlation energies E_{xc}^0 and E_{xc}^∞ are shown in Figs. 2 and 3 respectively. μ_h and μ_c are given in exciton Rydbergs (1 Ry = 2.655 meV) and are measured from the respective stressed band gaps.

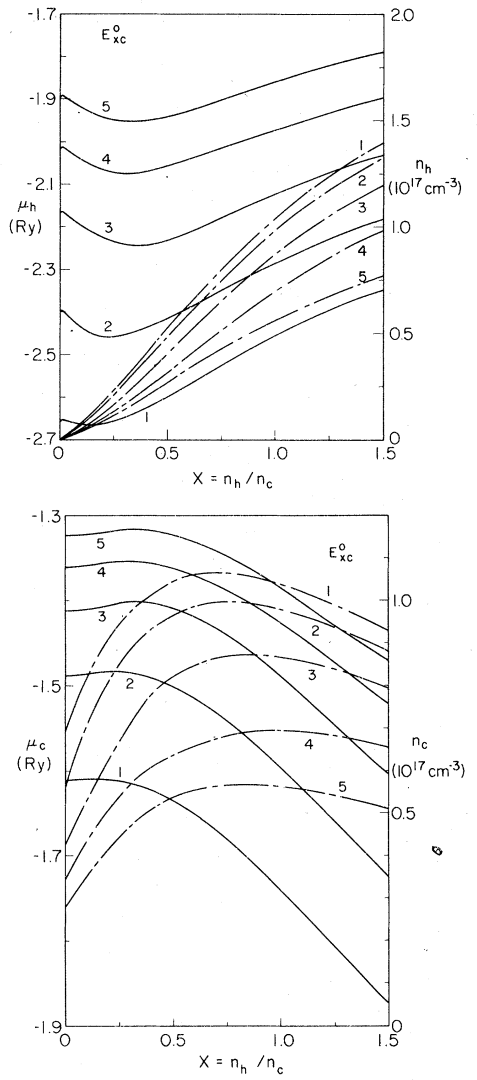

FIG. 2. (a) μ_h in exciton Rydbergs (solid curves) and n_h (broken curves) versus x at $T = 0$ and $p = 0$, for the model exchange-correlation energy E_{xc}^0 at different values of stress. Each curve is labeled by the value of the stress splitting (in meV) of the valence band at the center of the Brillouin zone. The stress values labeling the μ_h curves are near the left-hand side of the figure while those labeling the n_h curves are on the right: 1 Ry = 2.655 meV. (b) μ_c (solid curves) and n_c (broken curves) versus x at $T = 0$ and $p = 0$, for the model exchange-correlation energy E_{xc}^0. Each curve is labeled by the value of the stress splitting (in meV) of the valence band at the zone center. The stress labels of the μ_c curves are near the left side of the figure and those of the n_c curves are on the right.

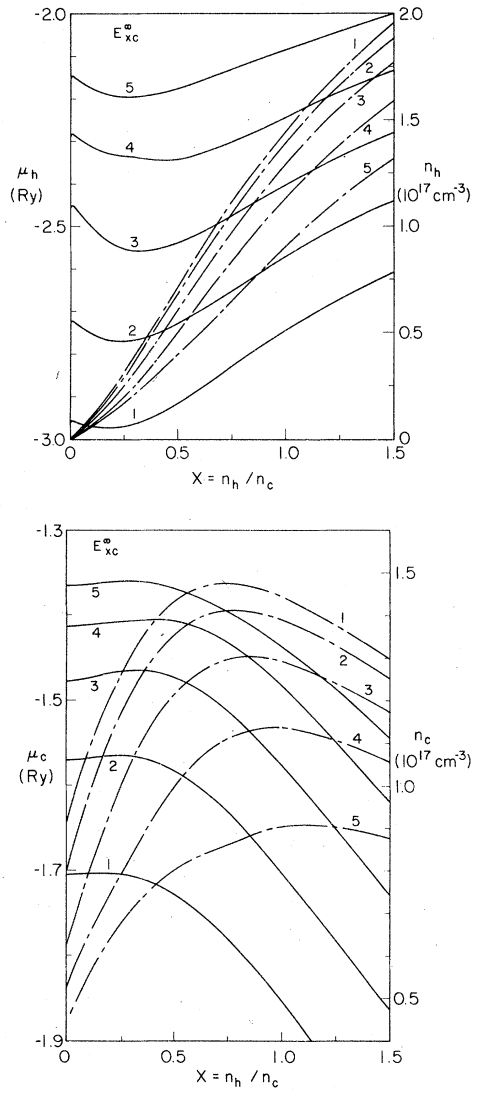

FIG. 3. (a) μ_h and n_h versus x at $T=0$ and $p=0$ for the model exchange-correlation energy E^{∞}_{xc}. Notation as in Fig. 2(a). (b) μ_c and n_c versus x at $T=0$ and $p=0$ for the model exchange-correlation energy E^{∞}_{xc}. Notation as in Fig. 2(b).

All of the curves for μ_h shown are of the type (b) of Fig. 1, i.e., all of them exhibit a minimum as a function of x so that a phase separation of the EHD is predicted. The corresponding chemical potential curves for the two different exchange-correlation energy models are very similar. They differ by a nearly rigid shift in energy. The small "lip" in each of the μ_h curves near $x=0$ is due to the $n_h^{2/3}$ contribution from the hot electron kinetic energy as discussed in the Appendix. The minimum in the hot pair chemical potential which is responsible for the phase separation of the EHD is most pronounced at intermediate stress values. It becomes very shallow at high and low stress. At very high stresses not shown in the figures it disappears completely and there is no phase separation. At very low stress we were not able to establish conclusively whether the minimum disappears completely or just becomes extremely shallow. The behavior of the hot and cold electron densities is also qualitatively very similar in the two models. These densities are somewhat higher for the model E^{∞}_{xc} than for E^{0}_{xc}.

From the discussion in Sec. II it follows that if the ratio N_h/N_c of hot to cold electrons in the system is less than x_c (where x_c is a critical concentration depending on the stress) the EHD separates into two phases which we will label I and II. Phase I has concentration $x=0$ (i.e., it contains no hot electrons) while in phase II the concentration equals x_c. The electron densities and chemical potentials in the two phases for any given stress can be read off at $x=0$ and $x=x_c$ in Figs. 2 and 3.

If the ratio N_h/N_c of hot to cold electrons in the system is greater than x_c then the EHD is uniform, there is no phase separation, and its hot and cold electron densities and chemical potentials are those shown for the value of x equal to N_h/N_c. (Of course the curves in Figs. 2 and 3 apply only when the EHD does not fill the entire crystal, since otherwise the condition $p=0$ need not be satisfied.)

To find the value of x_c for any given stress one may apply to μ_h the Maxwell construction discussed in Sec. II. Or, equivalently, one may just use the condition $\mu_c(x=x_c)=\mu_c(x=0)$, with the chemical potentials evaluated at $p=0$. [It is not necessary to consider μ_h explicitly so long as $\mu_h(x=0) > \mu_h(x=x_c)$.]

In Table I we list values of x_c for various values of stress and also the total electron density n in phases I and II for the two model exchange-correlation energies. [The Gibbs phase rule implies that if the two liquid phases are in equilibrium with each other and the temperature and pressure are fixed (e.g., $T=0$, $p=0$) then the total electron density and concentration of each phase are uniquely determined.]

Note that the density n_{I} of phase I is just the density at $T=0$ of the EHD which does not contain any hot electrons. In the range of stress values given in Table I this is the same as the density of the EHD in the "equilibrium limit" discussed in Ref. 15.

The qualitative aspects of the phase separation of the EHD can be understood intuitively in terms of the influence of the band structure of $\langle 111\rangle$-stressed Ge on the electron and hole kinetic energy. If we consider a uniform EHD (consisting of a single phase) in which there are many more cold electrons than hot electrons, the equilibrium density of such a uniform drop (and thus the exchange-

TABLE I. Total electron density (sum of hot and cold electron densities) $n_{\rm I}$ of phase I and $n_{\rm II}$ of phase II, and concentration $x_c = n_h/n_c$ for phase II of the EHD at $T=0$. The concentration x of phase I is zero. S_H is the stress-induced splitting of the valence band at $\vec{k}=0$. It is assumed that the EHD does not occupy the entire crystal so that $p=0$. The *numerical* accuracy of x_c and $n_{\rm II}$ depends on how pronounced the minimum in the μ_h curve is (Figs. 2 and 3), but is typically ~10%. The numerical accuracy of $n_{\rm I}$ is much better than this because a less delicate calculation is involved.

	E_{xc}^{∞}			E_{xc}^{0}		
S_H (meV)	x_c	$n_{\rm I}$ (10^{16} cm^{-3})	$n_{\rm II}$	x_c	$n_{\rm I}$ (10^{16} cm^{-3})	$n_{\rm II}$
1.5	0.31	8.7	16.6	0.28	6.4	11.8
2.0	0.38	8.0	17.6	0.37	5.6	12.5
2.5	0.46	7.1	18.5	0.47	4.7	13.1
3.0	0.54	6.2	19.0	0.54	4.2	12.8
3.5	0.60	5.7	18.6	0.54	3.8	11.3
4.0	0.60	5.3	16.9	0.48	3.4	9.4
4.5	0.46	4.9	12.3	0.50	3.1	8.8
5.0	0.45	4.5	11.4	0.53	2.8	8.3

correlation energy per electron-hole pair) will be determined primarily by the properties of the cold electrons. However, the hot electrons are distributed among three different conduction valleys while the cold electrons are confined to a single one. This reduces the hot electron kinetic energy in comparison with that of the cold electrons. If the number of hot electrons in the EHD is relatively small this tends to favor condensation of the hot electrons into a volume which is smaller than that which is "optimal" for the cold electrons. Whether a condensation of the hot electrons into a restricted part of the region occupied by the cold electrons is actually to occur is determined by a balancing of the contributions of the hot and cold electron kinetic energy, the hole kinetic energy, and the exchange-correlation energy. Our results indicate that the hole kinetic energy, which is the only one of these contributions which we take to be explicitly stress dependent,[24] is the deciding factor. At very large and very small stresses the extra hole kinetic energy which would be gained is sufficient (or very nearly sufficient in the low stress case) to prevent such a condensation from taking place. However, at intermediate stresses where the hole Fermi level is close to the valence band splitting, the hole density of states near to the Fermi level is strongly enhanced by the stress-induced valence-band nonparabolicity and by the presence of the deeper stress split valence band. This effect (which is absent at very large and very small stress) reduces the hole kinetic energy cost of condensation making the phase separation possible. The strong enhancement by valence band nonparabolicity of the density and binding energy of the EHD when no hot electrons are present was pointed out by Liu.[25] The underlying importance of the low kinetic energy of the hot electrons explains why in the present calculation (unlike the Hartree-Fock case) the phase separation occurs at $T=0$ only when the number of hot electrons in the system is smaller than the number of cold electrons.

Further insight into the nature of this two-component EHD system can be gained by plotting its $T=0$ phase diagram. Let $\bar{n}_h$ and $\bar{n}_c$ be the hot and cold electron densities *averaged over the entire crystal*. If the crystal contains two liquid phases I and II and a vapor phase (which we will label v), let the volumes occupied by these three phases be $\Omega^{\rm I}$, $\Omega^{\rm II}$, and Ω^{v} respectively, and let the hot and cold electrons densities in the three phases be labeled $n_h^{\rm I}$, $n_h^{\rm II}$, n_h^{v}, $n_c^{\rm I}$, $n_c^{\rm II}$, and n_c^{v}. Then

$$\bar{n}_h = \frac{n_h^{\rm I}\Omega^{\rm I} + n_h^{\rm II}\Omega^{\rm II} + n_h^{v}\Omega^{v}}{\Omega^{\rm I}+\Omega^{\rm II}+\Omega^{v}}\,,$$
$$\bar{n}_c = \frac{n_c^{\rm I}\Omega^{\rm I} + n_c^{\rm II}\Omega^{\rm II} + n_c^{v}\Omega^{v}}{\Omega^{\rm I}+\Omega^{\rm II}+\Omega^{v}}\,. \qquad (20)$$

Since $\bar{n}_h$ and $\bar{n}_c$ are proportional to the total numbers of hot and cold electrons present in the system, it is useful to classify $\bar{n}_c$-$\bar{n}_h$ space into regions in which different combinations of phases can coexist. This is done for $T=0$ and a valence-band stress splitting S_H of 3 MeV in Fig. 4. The

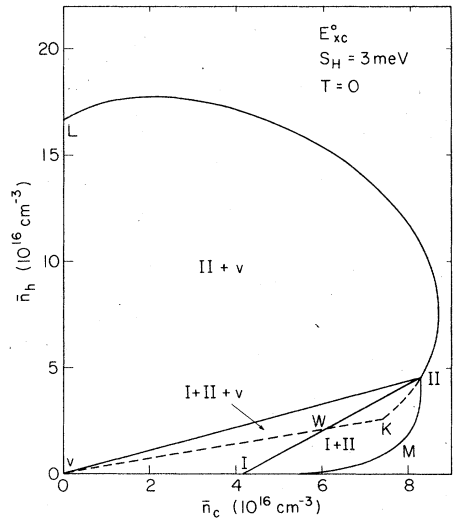

FIG. 4. Phase diagram of the two-component electron-hole liquid at $T=0$ and for a valence-band stress splitting of 3 meV. The model exchange-correlation energy E_{xc}^{0} was used. $\bar{n}_h$ and $\bar{n}_c$ are the densities of hot and cold electrons respectively averaged over the entire crystal. For an explanation of the nature of the various regions see text.

values plotted are for E^0_{xc}.

From (20) it follows that the region in $\bar{n}_c$-$\bar{n}_h$ space in which the three phases I, II, and v coexist is a triangle whose vertices have the coordinates (n_c^v, n_h^v), $(n_c^{\rm I}, n_h^{\rm I})$, and $(n_c^{\rm II}, n_h^{\rm II})$. In Fig. 4 we label these vertices v, I, and II respectively. Since at $T=0$ the vapor is the vacuum (by which we mean that there are no electrons or holes present), v is the point (0, 0). For thermodynamic states within the triangle v-I-II the EHD in its lowest-energy state consists of the two liquid phases and does not occupy the entire crystal. The densities and concentrations of the two liquid phases are those given in Table I. In the region bounded by the curve L-II and the straight line v-II, the EHD consists of a single liquid phase II in contact with vacuum. In the region bounded by the straight line I-II and the curve I-M-II the EHD consists of two liquid phases I and II and fills the entire crystal, i.e., the pressure is >0. In this region each of the liquid phases contains both hot and cold electrons, and in such cases we refer to the phase with the smaller value of x as phase I. The remainder of the phase diagram corresponds to the crystal completely filled with a homogeneous electron-hole liquid. In this region of the phase diagram it is possible to move from the point II to the point I by continuously varying the EHD density and concentration.

In the region bounded by the straight lines v-K and v-II, and by the curve II-K, it is also possible for the system to be in a metastable state. This state corresponds to a homogeneous EHD occupying part of the crystal, the remainder of the crystal being occupied by the vacuum. The possible densities of the hot electrons (n_h) and of the cold electrons (n_c) in this metastable homogeneous liquid phase are given by the coordinates (n_c, n_h) of the points of the curve II-K. Since this metastable region corresponds to zero pressure, the hot and cold electron densities and pair chemical potentials of the liquid phase which is present are given by portions of the $S_H = 3$ meV curves plotted in Figs. 2(a) and 2(b). The values of x which can be taken by the metastable liquid phase range from $x = x_{\rm min} \simeq 0.36$ (where the curve of μ_h versus x has its minimum) to $x = x_c \simeq 0.54$. For $x > x_c$, the homogeneous liquid at $p = 0$ is stable since no separation into two liquid phases is possible. For $x < x_{\rm min}$, $(\partial \mu_h/\partial x)_{p=0,\,T=0} < 0$ (except when x is very close to zero). This violates the thermodynamic stability conditions for a two-component system.[26] If a homogeneous electron-hole droplet is in some way prepared in the crystal in the range where $(\partial \mu_h/\partial x)_{p,T} < 0$, then any arbitrarily small fluctuation in local concentration $x_{\rm local}$ within the drop will grow rapidly, resulting in a spontaneous phase separation of the EHD. On the other hand, in the metastable region where $(\partial \mu_h/\partial x)_{p,T} > 0$, very small fluctuations in the local concentration $x_{\rm local}$ tend to damp out, so that a nucleation process must take place before the phase separation can occur, i.e., in the region where $(\partial \mu_h/\partial x)_{p,T} > 0$ only a concentration fluctuation greater than a certain critical magnitude can lead to a spontaneous phase separation of an EHD which has been prepared initially as a homogeneous liquid. How such a situation may arise experimentally will be discussed below. There is another very small region located close to the $\bar{n}_c$ axis in the phase diagram where metastable states can occur. This is related to the region of very small values of x in Fig. 2(a) where $(\partial \mu_h/\partial x)_{p=0,\,T=0}$ is positive. We do not depict that region explicitly in Fig. 4. Thus, in most of the triangular region v-W-I of the phase diagram, even a metastable EHD consisting of a single phase cannot occur. If a uniform EHD with parameters corresponding to this region were prepared it would be unstable and any arbitrarily small fluctuation would grow and lead to a phase separation.

We now apply this discussion to a possible experimental situation. Consider a stressed Ge crystal at a temperature which is low enough that the $T=0$ results apply. Suppose that this system is excited by a short laser pulse and that the photon frequency ν of the pulse is such that $h\nu$ is considerably larger than the band gap. Then most of the electrons which are excited into the conduction band by this laser pulse will appear in the conduction band at an energy well above the conduction band minimum. Thus, they will be equally likely to decay by emitting phonons into each of the four Ge conduction valleys, i.e., very soon after the laser pulse, the electron-hole system will be characterized by a concentration $x = N_h/N_c \simeq 3$. Then over a longer period of time lasting several microseconds the hot electrons will decay into the cold valley, i.e., we can think of the EHD forming with a concentration x near 3, this being followed by a period during which the value x decreases to near zero. This means that the EHD will be formed in the region labeled II + v in Fig. 4 (and fairly close to the origin unless the EHD fills a large fraction of the crystal). In this region the electron-hole liquid consists of a single phase. Then, as the hot electrons decay into the cold valley, the system will cross the line v-II and enter into the region of the phase diagram where, although the most stable state of the system is an EHD separated into the phases I and II, a uniform EHD can exist in a metastable state. In this region the transition from the uniform drop to the phase-separated one must proceed via a nucleation process. It is at present not known

how long such a process would take. It is possible that the uniform metastable EHD may persist long enough that the system crosses the line v-W of the phase diagram, because of the continuing decrease in the value of x. If this happens the uniform EHD ceases to be even metastable, and the time which it takes for the EHD to phase-separate will no longer be determined by a nucleation time but by the relatively short time it takes for the electrons to diffuse into the phase-separated configuration.[27]

Actual experimental identification of the phase separation could be carried out by the fitting of the EHD luminescence spectra to the line shapes which one would expect for a homogeneous and a phase-separated EHD. Alternatively, because of the large difference in density predicted for the two liquid phases (see Table I), one could look for two lines in the EHD plasmon absorption spectrum. Another method, which is a difficult but very direct one, would be to form a large EHD containing both hot and cold electrons and to attempt to observe the phase boundary directly by means of a spatial scan.

IV. BEHAVIOR AT FINITE TEMPERATURES

We generalize the treatment of the preceding section to the finite-temperature case as follows. The free energy of the electron-hole liquid can be written in the form

$$F(N_h, N_c, N_H, V, T) = F_h^0(N_h, V, T) + F_c^0(N_c, V, T) + F_H^0(N_H, V, T) + F_{xc}(N_h, N_c, N_H, V, T), \tag{21}$$

where F_i^0 is the free energy of noninteracting particles of species i, and F_{xc} is the exchange-correlation free energy. We approximate F_{xc} by its zero-temperature value E_{xc}. This approximation has been found to work very well in the case of the one-component EHD, both in unstressed semiconductors[19,28] and in ⟨111⟩-stressed Ge.[20] As in the zero-temperature case, we take $E_{xc}/(N_h+N_c)$ to depend only on the total density of hot and cold electrons. Then the expressions (8) for the hot and cold pair chemical potentials and for the pressure remain valid for $T>0$ if we extend to finite temperatures our definition of μ_i^0 and P_i^0 through

$$\mu_i^0 = \left(\frac{\partial F_i^0}{\partial N_i}\right)_{V,T}, \quad p_i^0 = -\left(\frac{\partial F_i^0}{\partial V}\right)_{N_i,T}. \tag{22}$$

In evaluating μ_i^0 and p_i^0 we do *not* make the commonly used approximation of replacing F_i^0 by the leading terms of a low-temperature expansion in powers of T^2. Such an approximation should not be used for the present system for two main reasons:

(i) It results in an unphysical singular behavior of the pair chemical potentials when the EHD density is such that the hole Fermi energy is close in magnitude to the size of stress-induced splitting of the valence band at $\vec{k}=\vec{0}$.

(ii) It also fails when $x=N_h/N_c$ is small, since then the degeneracy condition for the hot electrons that $kT/E_F(h)\ll 1$, where $E_F(h)$ is the hot electron Fermi energy, is not satisfied.

We are interested in both of these situations in which the T^2 expansion fails. Thus we evaluate μ_i^0 and p_i^0 exactly taking full account of the finite-temperature Fermi distribution.

For the electrons we use the exact finite-temperature Fermi expressions

$$n_e = \frac{\alpha_e}{2\pi^2}\left(\frac{2m_d}{\hbar^2}\right)^{3/2}\beta^{-3/2}\int_0^\infty \frac{Z^{1/2}dZ}{\exp(Z-\beta\mu_e^0)+1}, \tag{23}$$

$$p_e^0 = \frac{\alpha_e}{3\pi^2}\left(\frac{2m_d}{\hbar^2}\right)^{3/2}\beta^{-5/2}\int_0^\infty \frac{Z^{3/2}}{\exp(Z-\beta\mu_e^0)+1}, \tag{24}$$

where $\beta=1/kT$, the subscript e stands for h or c, and $\alpha_h=3$, $\alpha_c=1$. By inverting (23) numerically we obtain μ_e^0 as a function of n_e and T and then from (24) we have p_e^0 as a function of n_e and T.

Our choice of approximation for the exchange-correlation energy together with the use of the exact finite-temperature expressions (23) and (24) guarantees that the chemical potentials μ_h and μ_c which we calculate behave in a reasonable way even in the limit when the concentration of either the hot or cold electrons in the EHD becomes very low, provided that the density of the other electron species remains in the metallic range. For example, in the limit when $N_h/N_c\to 0$ the correct asymptotic behavior of dilute solutions[29] that

$$\mu_h \sim kT\ln\left(\frac{N_h}{N_c}\right) + \psi(p,T) \tag{25}$$

is ensured.

Expressions (23) and (24) are correct for parabolic bands. For the holes we use the corresponding finite T expressions for nonparabolic bands which can be written as

$$n_H = \beta\int_0^\infty \frac{E^{3/2}f_n(E/S_H)\exp[\beta(E-\mu_H^0)]dE}{\{\exp[\beta(E-\mu_H^0)]+1\}^2}, \tag{26}$$

$$p_H^0 = \int_0^\infty \frac{E^{3/2}f_n(E/S_H)dE}{\exp[\beta(E-\mu_H^0)]+1}. \tag{27}$$

The particular form given here is convenient to use because the same function f_n as was used in Sec. III [Eq. (12)] is involved. For the special

case of parabolic bands f_n is a constant and in that case (26) and (27) reduce to expressions having the same form as (23) and (24).

We calculate μ_{xc} and p_{xc} as in Sec. III. We would like to use as realistic a model for the exchange-correlation energy as we can, and for this reason we will work with the model E_{xc}^0. Experiments have been done measuring the electron-hole liquid densities in Ge as a function of stress at low temperatures in the equilibrium limit [which is explained in Sec. I (Refs. 21 and 22)]. The theoretical densities calculated from the model E_{xc}^0 for $T=0$ are in very good agreement with these experimental values throughout the entire range of stress values, whereas the densities obtained from E_{xc}^∞ are consistently too high.[15] The other available experimental tests of the model are the values of the critical temperature of the electron-hole liquid which have been measured at zero stress and at finite stress in the equilibrium limit. At zero stress we find an EHD critical temperature for the model E_{xc}^0 of approximately 8.7°K which is in satisfactory agreement with both experiment and other computational values.[1] Only a single measurement of the critical temperature of the EHD in the equilibrium limit is available for uniformly ⟨111⟩-stressed Ge, and the value obtained involved a considerable amount of extrapolation.[30] We find that the model E_{xc}^0 for the exchange correlation energy yields good agreement with experiment in this case also.

At finite temperatures it is possible to have two electron-hole liquid phases and a vapor phase simultaneously present and in equilibrium with each other. We will refer to such a situation as three-phase equilibrium. Our major aim is to predict under what conditions three-phase equilibrium is expected to occur. The method which we use depends on the temperature range which is being considered because the nature of the vapor phase is different at high and low temperatures.

(a) At low temperatures the vapor phase consists of excitons containing electrons of the two species. Neither the binding energy of the "hot" and "cold" free excitons nor their dispersion (i.e., the $\vec{k}$ dependence of their translational masses) in stressed Ge is known theoretically, and only rather approximate binding energies are available experimentally. For this reason it is not possible at present to calculate meaningful values for the density and concentration of the vapor which is in equilibrium with the two liquid phases in this temperature regime. However, the properties of the two liquid phases under conditions of three-phase equilibrium can still be calculated. This is because at low temperatures the pressure of the vapor phase is very low so that we can set it equal to zero. Thus, at low temperatures we calculate μ_h, μ_c, and n as a function of x at $p=0$ and at fixed temperature T. This is done by the same procedure as described in Sec. III for the $T=0$ case, but using the finite T expressions (23), (24), (26), and (27). For values of stress at which the phase separation of the EHD is predicted to occur at zero temperature, the curves of μ_h versus x at constant $p(=0)$ and T obtained in this way are of the type (a) of Fig. 1, for low temperatures T. As the temperature is increased, the nonmonotonicity of these curves becomes less pronounced. In some cases the μ_h versus x curve becomes monotonic while the temperature is still in the range in which the $p=0$ approximation is valid. Having evaluated μ_h, μ_c, and n as a function of x at $p=0$ and constant T, it is easy to find the values of x and n in the two coexisting liquid phases I and II by solving

$$\mu_h^{\mathrm{I}}=\mu_h^{\mathrm{II}},$$

$$\mu_c^{\mathrm{I}}=\mu_c^{\mathrm{II}},$$

subject to the constraint $p=0$, at any temperature at which such solutions exist.

The validity of the $p=0$ approximation can be checked by estimating the actual pressure of the exciton vapor from the classical expression

$$p_{\mathrm{classical}}=\sum_i g_i(kT)^{5/2}\left(\frac{m_i}{2\pi\hbar^2}\right)^{3/2}e^{-\beta\phi_i}, \qquad (28)$$

where g_i is the degeneracy and m_i the translational mass of the exciton of species i, and ϕ_i is the binding energy of the EHD relative to the free exciton of species i. We estimated (28) as follows: In practical situations the quantity ϕ_i is much larger for excitons involving hot electrons than cold electrons because of the much higher Fermi energy of the cold electrons in the EHD. For this reason at low temperatures as a first approximation the contribution of hot free excitons to the exciton pressure can be neglected. Thus we calculated only the contribution of the cold free excitons to the exciton pressure using (28). The experimental value[31] of ϕ for cold free excitons relative to the EHD at $x=0$ and $T=2.08$°K was used as a reference point in calculating the value of ϕ for cold free excitons at other values of T and x. A rough estimate was made for m_i, noting that $p_{\mathrm{classical}}$ is not very sensitive to this parameter. The values of μ_h, μ_c, n, and x in the two coexisting liquid phases were recalculated setting $p=p_{\mathrm{classical}}$ instead of $p=0$. Since μ_c enters into the expression for $p_{\mathrm{classical}}$ through ϕ, $p_{\mathrm{classical}}$ and μ_c were calculated self-consistently. It was found as expected that in the low-temperature regime replacing the ansatz $p=0$ by p

$=p_{\text{classical}}$ has no significant effect on the values of x and n obtained for the two coexisting liquid phases.

(b) At higher temperatures as pointed out by Combescot,[19] the vapor phase which is in contact with the electron-hole liquid becomes metallic, and is thus correctly described by the same approximations which are used to treat the liquid phases. Thus we calculate μ_h, μ_c, and p for both liquid phases and for the vapor from the expressions (8), (10), (23), (24), (26), and (27). This approach is believed to be valid provided that the density of the vapor is not too low.[1] A crude estimate of the density above which the method is expected to be meaningful is given by equating the Debye-Huckel screening length in the vapor to the exciton Bohr radius. This yields a density

$$n_{\text{DH}}=\frac{1}{16\pi}\frac{kT}{\text{Ry}\,a_0^2}, \tag{29}$$

where Ry is the exciton Rydberg and a_0 the exciton Bohr radius. n_{DH} depends on the temperature but is typically $\lesssim 10^{15}/\text{cm}^3$ if we take a_0 to be 177 Å. This density is considerably lower than the vapor densities with which we work at high temperatures.

As the temperature increases, the calculation becomes progressively a more delicate one. This is because the features of the curves of μ_h and μ_c versus x at constant p and T which are responsible for the phase separations are much less pronounced at high temperatures than at low temperatures. For this reason the detailed results obtained from our simplified exchange correlation energy at high temperatures can be expected to be less reliable than our zero-temperature predictions. However, as has already been mentioned in the Introduction, comparison of the results obtained from the two different choices of correlation energy (SPH and Hubbard) which we studied is somewhat encouraging.

There is also the separate matter of numerical accuracy. Since we calculate μ_i^0 and p_i^0 directly from expressions (23), (24), (26), and (27), these quantities are evaluated quite accurately with an estimated numerical error ~0.1%. However p_{xc} and μ_{xc} are obtained by the procedure given in Sec. III. This involves numerically interpolating and differentiating the correlation energy which enters into E_{xc}^0 and which is known numerically only with a limited accuracy. Because of this, the numerical values which we obtain in the high-temperature region are sensitive to the choice of interpolation procedure for the correlation energy. However, the *qualitative* features of the phase diagrams which we obtain are not.

The method which we use to solve for three-phase equilibrium at high temperatures is illustrated in Fig. 5, where we show some typical plots of μ_h versus x at constant T and p. The breaks in the μ_h curves are due to unstable states (which are not shown) for which $(\partial p/\partial V)>0$. The corresponding plots of μ_c versus x are very similar qualitatively to the μ_h curves except that all of the lines have slopes of the opposite sign so that the curves appear inverted. The density n which corresponds to a particular isobar generally increases with increasing x so that the portions of the curves in Fig. 5 which occur to the left of the break can be identified as corresponding to the vapor while those to the right correspond to the liquid.

To establish whether phase equilibrium is possible between two or more phases at a given value of T and p, one must determine whether it is possible for μ_h as well as μ_c to be simultaneously the same in all phases. We begin by solving iteratively the equations

$$\mu_h^\alpha=\mu_h^\beta,$$
$$\mu_c^\alpha=\mu_c^\beta$$

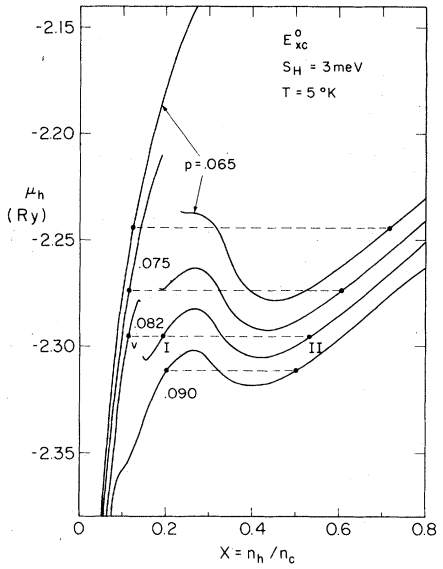

FIG. 5. μ_h versus x at constant temperature and pressure for $T=5$ °K, $S_H=3$ meV and the exchange-correlation energy E_{xc}^0. The curves are labeled by the value of the pressure in units of 10^{-22} Ry m^{-3}. A break occurs in some of the curves because we only plot states for which $(\partial p/\partial V)_{N_h,N_c,N_H,T}<0$. The scale of μ_h values shown applied to the curve labeled $p=0.065$. The remaining curves have been displaced successively to lower energies by increments of 0.01 Ry in order to separate them. Three-phase equilibrium occurs at $p\simeq 0.082$. States which are in equilibrium with each other are indicated by solid circles joined by dashed lines.

for equilibrium between two phases α and β at a given pressure and then determine whether a third phase γ can coexist with α and β. We find, as expected from the Gibbs phase rule, that at a given (not too large) value of T, there is a continuum of values of p for which two phases can coexist, but that three phases can coexist only at a unique value of p. In Fig. 5 we indicate examples of coexisting phases by solid circles joined by dashed lines. At $p=0.065$ and 0.075 only coexistence between the vapor and one liquid phase is possible. At $p=0.090$ only two liquid phases (filling the entire crystal) can coexist. At $p\simeq 0.082$ the vapor (v) can coexist simultaneously with the two liquid phases I and II. That the two liquid phases can coexist at $p=0.082$ and 0.090 is obvious from Fig. 5 by itself since the Maxwell construction in μ_h-x space can be carried out. The liquid-vapor equilibrium can also be obtained from the Maxwell construction if the entire μ_h-versus-x curve is computed.

In Fig. 6 we give a more detailed map of the phase equilibria which can occur under the same conditions of temperature and stress as are considered in Fig. 5. The concentrations x of the pairs of phases which can coexist at any value of p can be read from Fig. 6 in the following way. Points on the lines F-J and corresponding points (at the same pressure) on line K-L give respectively the concentrations of the vapor and liquid phase II which can coexist with the vapor. In the same way lines Q-R and Q-S correspond respectively to the coexisting vapor and liquid phase I. Lines M-N and M-O give respectively the coexisting liquid phases I and II when the liquid fills the entire crystal. The points labeled v, I, and II give the vapor and liquid phases I and II respectively at three-phase equilibrium. The line segments F-v, v-R, N-I, I-S, K-II, and II-O appear to correspond to metastable states. The p-n diagram related to the p-x diagram in Fig. 6 can also be drawn. Its general appearance is very similar to Fig. 6, but we do not give it here, since a more transparent way of presenting the behavior of the system at fixed temperature is available.

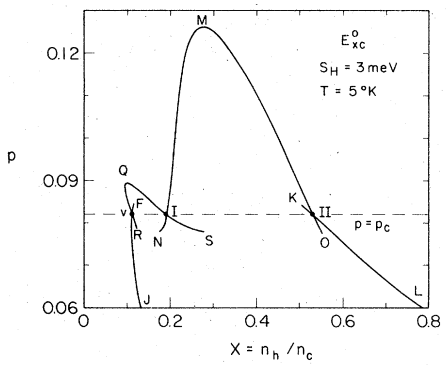

FIG. 6. The concentration x of the phases which can coexist at various pressures p (in units of 10^{-22} Ry m^{-3}) at a stress $S_H=3$ meV and temperatures 5 °K. The exchange-correlation model used is E^0_{xc}. Three-phase equilibrium occurs at $p=p_c$. The meaning of the various line segments is explained in the text.

In Fig. 7 we show the fixed-temperature section through the $\bar{n}_c$-$\bar{n}_h$-T-space phase diagram of the two-component electron-hole system, for $T=5$ °K and $S_H=3$ meV. This figure should be compared with Fig. 4 which is a similar section through the phase diagram but taken at $T=0$. The main qualitative difference between the two figures is that at 5°K the triangle v-I-II (in which we have three-phase equilibrium) has moved away from the $\bar{n}_c$ axis and from the origin so that the vapor phase v is no longer the vacuum. Also a new region v-I-Q has appeared in which we have vapor in equilibrium with liquid phase I. We do not show the regions in which metastable states are possible in Fig. 7. The boundary of region II + v has not been closed since part of it corresponds to vapor densities which are too low to be handled meaningfully by the present methods. In the region below the curve L-II-M-I-Q-v-J it is possible to go continuously from liquid phase II to liquid phase I to vapor.

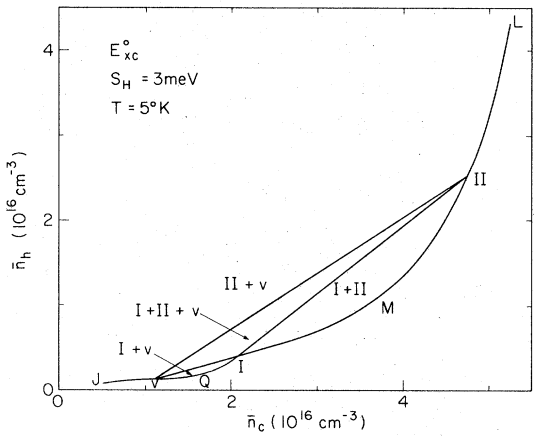

FIG. 7. Constant temperature section through the phase diagram of the two-component electron-hole system for $T=5$ °K, $S_H=3$ meV and the model E^0_{xc}. Corresponding states of Fig. 6 and Fig. 7 are labeled by the same symbols. The regions of the phase diagram are labeled according to the phases which they contain. The entire boundary of the region containing vapor (v) and liquid phase II in contact with each other is not shown in the figure (i.e., the way in which the curve J-v-II-L should close is not shown) because this would involve extending the calculation to too low a vapor density.

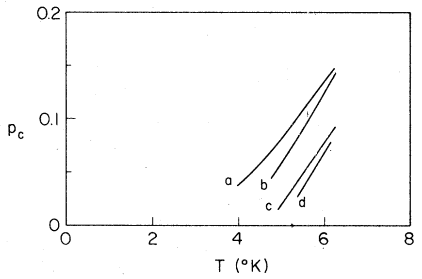

FIG. 8. The pressure p_c (units of 10^{-22} Ry m^{-3}) at which three-phase equilibrium occurs as a function of temperature. *a*: $S_H = 3$ meV, E_{xc}^0; *b*: $S_H = 1.5$ meV, E_{xc}^0; *c*: $S_H = 3$ meV, Hubbard; *d*: $S_H = 2$ meV, Hubbard. The exchange-correlation energies E_{xc}^0 and Hubbard refer to the SPH and Hubbard values for the model band structure (i) described in the Introduction.

As the temperature is varied, the region of the $\bar{n}_c$-$\bar{n}_h$ plane in which three-phase equilibrium is found changes, as does the pressure p_c at which three-phase equilibrium occurs. Plots of p_c versus temperature for different values of stress and for two choices of the exchange-correlation energy are given in Fig. 8.

The information which is required to delineate the region of the phase diagram in which three-phase coexistence occurs is contained in a compact form in the coexistence curves for three-phase equilibrium. These are given for three different values of stress for the exchange-correlation energy E_{xc}^0 in Figs. 9(a), 9(b), and 9(c). We have plotted as a function of T the values of x and n which the two liquid phases and the vapor have when all three phases are in equilibrium. The values for the vapor are plotted only in the higher temperature region in which method (b) above is used for the calculation. The dotted lines are a smooth interpolation between the high and low T regions. Since in Fig. 9 we are concerned only with three-phase equilibrium, some of the lines which we have plotted terminate abruptly when the temperature rises into a range in which three-phase equilibrium is not possible. Given x and n for each of the three phases in equilibrium as a function of the temperature, the region of the phase diagram in $\bar{n}_c$-$\bar{n}_h$-T space in which three-phase coexistence occurs can be found by constructing its constant-T sections according to the method in Sec. III.

Figures 9(a), 9(b), and 9(c) show that the system behaves differently as the temperature rises for different values of stress. In Fig. 9(a) ($S_H = 4$ meV) we have two liquid phases I and II at low temperatures which dissolve in each other at a critical temperature of solution between 3 and 4 °K. In the language of Fig. 7 this can be viewed as follows: The side I-II of the triangle in $\bar{n}_c$-$\bar{n}_h$ space which forms the constant-temperature cross section of the three-phase region of the phase diagram degenerates into a point as the temperature rises. Thus, the triangle degenerates into a line and the three-phase region disappears as the temperature rises through the critical point of solution.

In Fig. 9(b) where the stress is lower ($S_H = 3$ meV) the behavior is quite different as the temperature is raised. As the temperature increases the liquid phase II continues to exist as a separate phase while the less dense liquid phase I and the vapor merge. At this stress as the temperature rises it is the side v-I of the triangle of Fig. 7 which degenerates into a point where the three-phase coexistence region terminates. The liquid-vapor critical point (6–7 °K) is difficult to study numerically and for that reason parts of the lines in Fig. 9(b) have been dashed.

At a stress $S_H = 1.5$ meV [Fig. 9(c)] the behavior of the coexistence curves is particularly interesting. At low temperatures we find two coexisting liquid phases which dissolve in each other at $T \sim 2$ °K. For $T \gtrsim 5$ °K we again find coexistence of two liquid phases and the vapor. As the temperature rises further the less dense liquid phase I and the vapor eventually merge. In the temperature range approximately 2–5 °K it is not possible to have two liquid phases simultaneously present, i.e., all of the μ_h isobars in this temperature range are monotonic functions of x in the entire region associated with the electron-hole liquid so that two liquid phases cannot coexist.

This remarkable low-stress behavior can be physically interpreted as follows. At very low temperatures the chemical potential μ_h as a function of x has a minimum which is responsible for the phase separation. As the temperature increases, this minimum becomes shallower due to the contributions to μ_h of its temperature-dependent part which is roughly proportional to $-T^2/n_h^{2/3}$ and is a rapidly increasing function of x. Thus, the minimum in the μ_h versus x isobar eventually disappears as the temperature increases, and the two liquid phases coalesce. With further increase of temperature the EHL density begins to decrease rapidly. When the density has fallen to a point where the hole Fermi level is close to the valence band separation, the valence band nonparabolicity at the hold Fermi level is particularly strong. The stronger nonparabolicity of the valence band near to the hole Fermi level favors the phase separation of the EHD as explained in Sec. III. It appears that this effect offsets the contribution of the temperature-dependent part of μ_h which was described above, and the phase separation of the

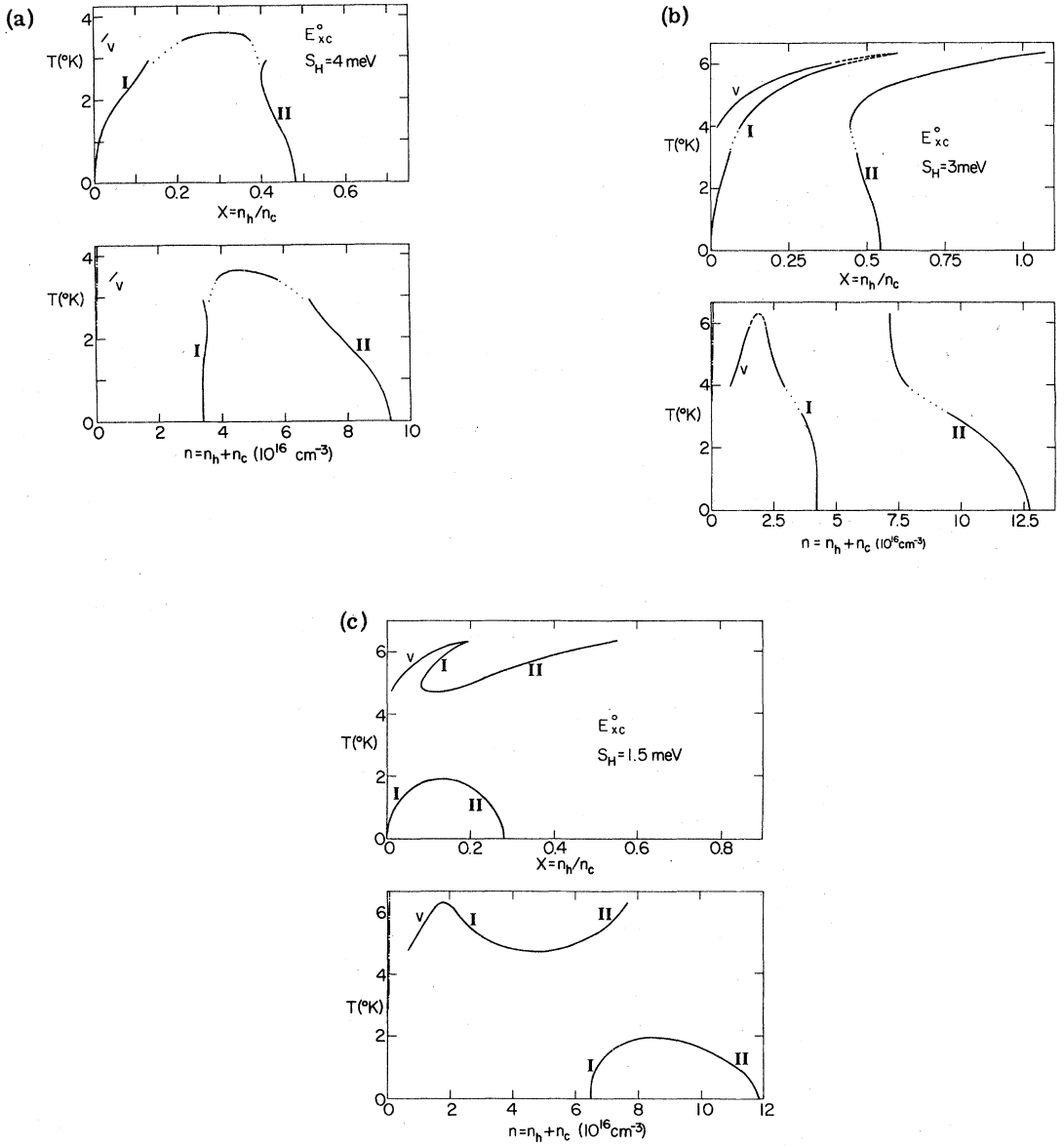

FIG. 9 (a) Coexistence curves for three phases in equilibrium, for a stress-induced valence band splitting at the zone center $S_H = 4$ meV. The values of the concentration x and total density n for each coexisting phase are plotted at various temperatures. E^0_{xc} is the exchange correlation energy used. The liquid phases are labeled I and II, and v denotes the vapor. The vapor phase is not plotted at low temperatures. Dotted lines are a smooth interpolation between the low and high T regions. The dot-dashed line denotes the density n_{DH} at which the Debye-Hückel screening length equals the exciton Bohr radius—see Eq. (29). (b) Coexistence curves for three phases in equilibrium for a valence band splitting $S_H = 3$ meV and the exchange-correlation energy E^0_{xc}. Notation as in (a). For explanation of the dashed lines see text. (c) Coexistence curves for three phases in equilibrium for a valence band splitting $S_H = 1.5$ meV and the exchange-correlation energy E^0_{xc}. Notation as in (a).

EHD reappears.

The information in Figs. 9(a)–9(c) can be presented in an alternative form by drawing the region of the phase diagram in $\bar{n}_c$-$\bar{n}_h$-T space in which three-phase coexistence occurs. This has been done for $S_H = 3$ meV and 1.5 meV in Figs. 10(a) and 10(b), respectively. The three-phase region of the phase diagram for $S_H = 4$ meV is similar to the lower part of Fig. 10(b).

In order to see how sensitive the remarkable behavior which we found at low stress is to the choice of the exchange-correlation energy we

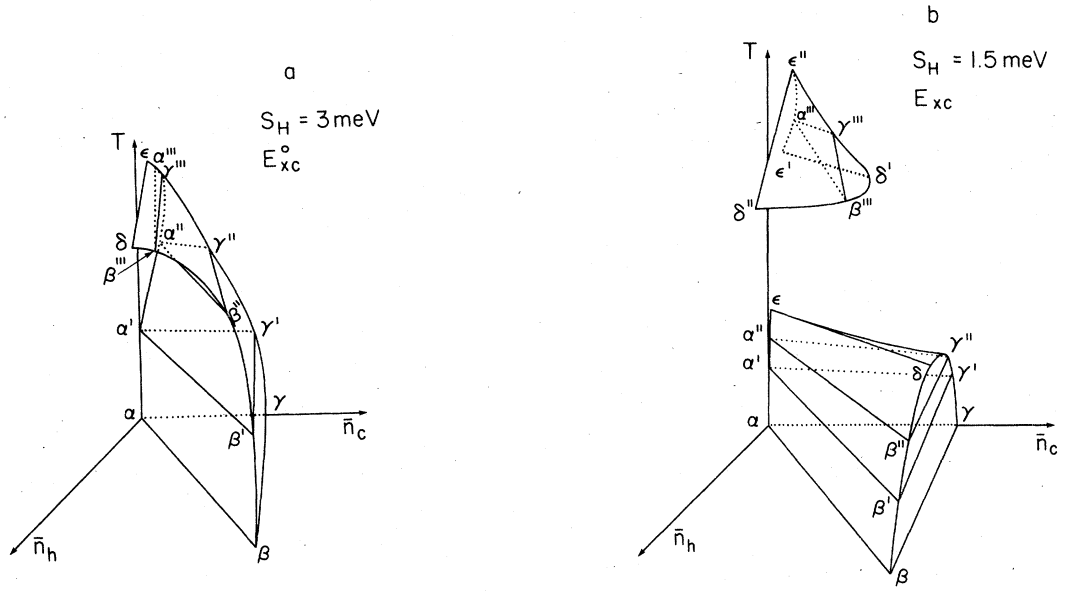

FIG. 10. Pictorial representation of the regions of the phase diagram in $\bar{n}_h$-$\bar{n}_c$-T space in which the two liquid phases and the vapor coexist. This is an alternative representation of the same information as is contained in the coexistence curves [(b) and (c)]. Because of the difficulties inherent in depicting solids in two dimensions, a detailed description is necessary: (a) The case of a valence band splitting of 3 meV for the model exchange correlation energy E^0_{xc}. At each fixed temperature the three-phase coexistence region is a triangle contained in a plane parallel to the $\bar{n}_h$-$\bar{n}_c$ plane. These triangles are shown explicitly for a number of arbitrarily chosen temperatures. The positions of three vertices (denoted α^i, β^i, and γ^i) of triangle i correspond to the entire system containing only the vapor or only the liquid phase II or only the liquid phase I respectively. As the temperature increases the vertices α^i and γ^i come closer together and finally merge into each other at the point ϵ, at the temperature at which the liquid phase I and the vapor become indistinguishable. At that temperature the triangle $\alpha^i\beta^i\gamma^i$ degenerates into the line $\epsilon\delta$. The line $\epsilon\delta$ is parallel to the $\bar{n}_h$-$\bar{n}_c$ plane. (b) The case of a valence-band splitting of 1.5 meV for the model exchange-correlation energy E^0_{xc}. The coexistence of three phases occurs in two disjoint regions. As in case (a), at each fixed temperature the three-phase coexistence region is a triangle with vertices $\alpha^i, \beta^i, \gamma^i$. In the lower temperature region of the phase diagram we begin at $T=0$ with a triangular cross section α-β-γ of the three-phase coexistence region. As the temperature increases, the vertices β_i and γ_i of the triangle i (which represent the liquid phases II and I respectively) come closer together in $\bar{n}_h$-$\bar{n}_c$ space and eventually merge at the point δ. At the temperature at which this takes place the triangle $\alpha^i\beta^i\gamma^i$ degenerates into the line $\epsilon\delta$ which is parallel to the $\bar{n}_h$-$\bar{n}_c$ plane. In the intermediate temperature range the simultaneous presence of all three phases is not possible. In the higher temperature range the three-phase coexistence region again has a triangular cross section at each fixed temperature. Such a representative triangle at one particular temperature T''' is labeled $\alpha'''\beta'''\gamma'''$ in the figure. As the temperature rises above T''' the vertices α^i and γ^i of the triangle come together and merge at the point ϵ'' while the vertex β^i approaches the point δ'', so that the triangle $\alpha^i\beta^i\gamma^i$ degenerates into the line $\epsilon''\delta''$ which is parallel to the $\bar{n}_h$-$\bar{n}_c$ plane, ie., the liquid phase I and vapor merge. At temperature below T''' the vertices β^i and γ^i of triangle i come together with decreasing temperature and merge at the point δ', while α^i approaches the point ϵ', i.e., the triangle $\alpha^i\beta^i\gamma^i$ degenerates with *decreasing* temperature into the line $\epsilon'\delta'$ which is parallel to the $\bar{n}_h$-$\bar{n}_c$ plane. In other words, the liquid phases I and II eventually become indistinguishable as the temperature decreases.

performed the above calculations at two values of stress using E_{xc} (Hubbard) instead of E^0_{xc}. The results are shown in Figs. 11(a) and 11(b), and are similar to those in Fig. 9(c). As can be seen in Fig. 8, the pressure p_c which corresponds to three-phase equilibrium is consistently lower if one uses E_{xc} (Hubbard) than if one uses E^0_{xc} for the exchange-correlation energy. For this reason it turns out to be necessary to use the zero-pressure approximation up to higher temperatures when the Hubbard correlation energy is used.

Comparison of Figs. 9 and 11 shows that while the reappearance of the phase separation at higher temperatures appears to survive modest changes in the exchange-correlation energy, a more detailed theory is needed in order to be able to make accurate predictions at high temperatures.

V. DISCUSSION

Our calculations have shown that the two-component electron-hole liquid in stressed Ge is a

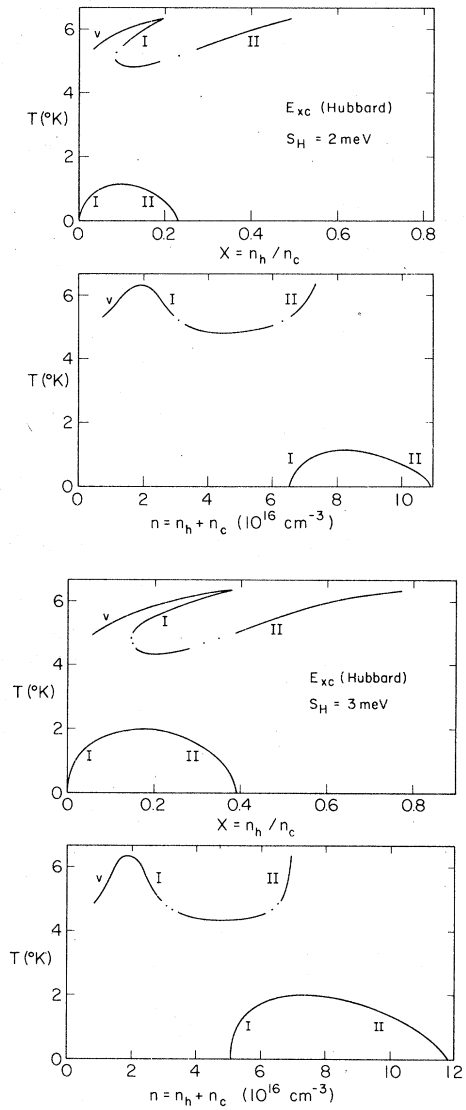

FIG. 11. (a) Coexistence curves for three phases in equilibrium for a valence-band splitting $S_H = 2$ meV, using the exchange-correlation energy E_{xc} (Hubbard). Notation as in Fig. 9. (b) Coexistence curves for three phases in equilibrium for a valence-band splitting $S_H = 3$ meV using the exchange-correlation energy E_{xc} (Hubbard). Notation as in Fig. 9.

system of considerable interest from the point of view of both theory and experiment. It is a unique case of a degenerate two-component Fermi system which can be studied in the laboratory. In addition, the magnitude of the stress applied to the crystal provides a crucial parameter in the Hamiltonian of the liquid which can be varied at will by the experimentalist.

The main approximation which has been made in our theory is that the exchange-correlation energy per electron-hole pair in the electron-hole liquid depends only on the total density of hot and cold electrons. At $T=0$ we have examined many models for the exchange-correlation energy having this property, in addition to those described in this paper. In all cases we found that the two-component electron-hole liquid phase separates in an intermediate stress range in a manner very similar to that described in Sec. III.

The Hartree-Fock approximation and related approximations in which an approximate correlation energy per pair (taken to depend only the total density of hot and cold electrons in the EHD) is added to the *exact* exchange energy (per pair) of the EHD, provide some examples of model exchange-correlation energies which depend on the way in which the electrons are distributed among the hot and cold valleys as well as on the total density. While all of these Hartree-Fock type models predict that the two component EHD should phase separate, they all suffer from the same inconsistencies as the Hartree-Fock approximation (Appendix) and thus should be considered as inferior to the models which we have used in this paper.

In a recent article, Feldman and Markiewicz[32] calculated the energy which is gained (per electron-hole pair) when the two-component electron-hole liquid phase separates at $T=0$. They found this energy to be quite small and concluded that this implies that the phase separation of the EHD would only occur at temperatures well below 2°K. Our explicit finite-temperature calculations show this conclusion to be invalid, and that the phase separation of the two-component EHD may well persist up to temperatures comparable with the liquid-vapor critical point. However, it is clear that only experiment will be able to determine unambiguously to what extent our predictions are correct.

ACKNOWLEDGMENTS

We thank J. Bajaj, H.-h. Chou, L. Liu, P. Vashishta, and G. K. Wong for helpful discussions. This work was supported in part under the N.S.F.-M.R.L. program through the Material Research Center of Northwestern University (Grant No. DMR 76-80847) and in part by the N.S.F. (Grant No. DMR 77-09937).

APPENDIX: DISCUSSION OF THE HARTREE-FOCK APPROXIMATION AT $T=0$

The exchange energy of the two-component EHD at $T=0$ can be written

$$E_x = -\gamma_h N_h n_h^{1/3} - \gamma_c N_c n_c^{1/3} - E_{xH} , \qquad \text{(A1)}$$

where a homogeneous electron-hole liquid has been assumed, γ_h and γ_c are positive constants, and E_{xH} is the hole exchange energy. In the limit of small $x = N_h/N_c$ the variation with n_h of the hot pair chemical potential μ_h, in the HFA, is dominated by the contribution

$$\frac{\partial}{\partial N_h}(-\gamma_h N_h n_h^{1/3})_V = -\tfrac{4}{3}\gamma_h n_h^{1/3} \tag{A2}$$

from the first term on the right-hand side of (A1), i.e., from the exchange interaction between the hot electrons. [The contribution to μ_h of the hot electron kinetic energy which is proportionai to $n_h^{2/3}$ is a much more slowly varying function of n_h (in the limit of small n_h) than the term (A2). The other Hartree-Fock contributions to μ_h are also more slowly varying.] This implies that for sufficiently small x,

$$\left(\frac{\partial \mu_h}{\partial x}\right)_{p,\,T=0} < 0\,, \tag{A3}$$

which is in violation of the thermodynamic stability requirements for a uniform two-component system.[26] Consequently, for very small values of x the EHD must phase separate in the HFA. A similar argument applied to μ_c shows that in the HFA the EHD must also phase separate if x is sufficiently large.

If correlation effects are included, the exchange interaction between hot electrons will be screened out in the limit $n_h \ll n_c$ and the variation of μ_h with n_h in the limit of small x will be dominated by the contribution from the hot electron kinetic energy, i.e.,

$$\mu_h - \mu_h(n_h = 0) \sim n_h^{2/3} \tag{A4}$$

in the limit of small n_h. Thus, the limiting HFA result (A3) fails when correlations are included. The result (A4) can be viewed as the extension to zero temperature for a Fermi system of the usual finite temperature asymptotic property of dilute solutions.[29]

This illustrates the need for a careful choice of the approximations used for the exchange-correlation energy of this system. Our use of exchange-correlation energies which depend only on the total electron density guarantees that the requirement (A4) is satisfied at $T = 0$.

---

*Present address: Department of Physics, Boston University, 111 Cummington Street, Boston, MA 02215.

[1]For a general review of electron-hole liquid theory and experiments prior to the observation of the "hot" electrons in the electron-hole drop see the articles by by T. M. Rice and by J. C. Hensel, T. G. Phillips and G. A. Thomas, in *Solid State Physics*, edited by H. Ehrenreich, F. Seitz, and D. Turnbull (Academic, New York, 1977), Vol. 32.

[2]H.-h. Chou, G. K. Wong, and B. J. Feldman, Phys. Rev. Lett. 39, 959 (1977).

[3]B. J. Feldman, H.-h. Chou, and G. K. Wong, Solid State Commun. 28, 305 (1979).

[4]H.-h. Chou, J. Bajaj, and G. K. Wong, J. Lumin. 18–19, 131 (1979).

[5]W. F. Brinkman and T. M. Rice, Phys. Rev. B 7, 1508 (1973).

[6]M. Combescot and P. Nozières, J. Phys. C 5, 2369 (1972).

[7]P. Vashishta, P. Bhattacharyya, and K. S. Singwi, Phys. Rev. B 10, 5108 (1974).

[8]P. Bhattacharyya, V. Massida, K. S. Singwi, and P. Vashishta, Phys. Rev. B 10, 5127 (1974).

[9]C. Ebner and D. O. Edwards, Physics Rep. 2C, 78 (1971).

[10]J. M. Kincaid and E. G. D. Cohen, *ibid.* 22C, 58 (1975).

[11]G. Baym and C. Pethick, Ann. Rev. Nucl. Sci. 25, 27 (1975).

[12]See for example J. M. Lattimer and D. G. Ravenhall, Astrophys. J. 223, 314 (1978).

[13]D. Q. Lamb, J. M. Lattimer, C. J. Pethick, and D. G. Ravenhall, Phys. Rev. Lett. 41, 1623 (1978).

[14]G. Kirczenow and K. S. Singwi, Phys. Rev. Lett. 41, 326 (1978); Phys. Rev. Lett. 41, 1140(E) (1978).

[15]G. Kirczenow and K. S. Singwi, Phys. Rev. B 19, 2117 (1979).

[16]G. E. Pikus and G. L. Bir, Fiz. Tverd. Tela (Leningrad) 1, 1828 (1959) [Sov. Phys.—Solid State 1, 136 (1959)].

[17]J. C. Hensel and K. Suzuki, Phys. Rev. B 9, 4219 (1974).

[18]G. Kirczenow and K. S. Singwi, Phys. Rev. Lett. 42, 1004 (1979); 42, 1315 (E) (1979).

[19]M. Combescot, Phys. Rev. Lett. 32, 15 (1974).

[20]L. Liu and L. S. Liu, Solid State Commun. 27, 801 (1978).

[21]H.-h. Chou and G. K. Wong, Phys. Rev. Lett. 41, 1677 (1978).

[22]G. A. Thomas and Ya. E. Pokrovskii, Phys. Rev. B 18, 864 (1978).

[23]An alternative derivation of (5) in which the holes are treated explicitly is given for $T = 0$ in Ref. 14.

[24]Since in our calculations the transitions between the hot and cold valleys are neglected, the value of the stress-dependent energy splitting of the hot and cold conduction valley minima does not enter.

[25]L. Liu, Solid State Commun. 25, 805 (1978).

[26]L. D. Landau and E. M. Lifshitz, *Statistical Physics*, second edition (Addison-Wesley, Reading, Mass., 1969), p. 298.

[27]A discussion of the theory of such processes in other systems is given by J. S. Langer, in *Fluctuations, Instabilities and Phase Transitions*, edited by T. Riste (Plenum, New York, 1975), p. 19.

[28]T. M. Rice, in *Proceedings of the Twelfth ICPS*, edited by M. H. Pilkuhn (Teubner, Stuttgart, 1974), p. 23.

[29]L. D. Landau and E. M. Lifshitz, *Statistical Physics*, second edition (Addison-Wesley, Reading, Mass., 1969) p. 277.
[30]B. J. Feldman, H.-h. Chou, and G. K. Wong, Solid State Commun. 24, 521 (1977).
[31]B. J. Feldman, H.-h. Chou, and G. K. Wong, Solid State Commun. 26, 209 (1978).
[32]B. J. Feldman and R. S. Markiewicz, Solid State Commun. 29, 411 (1979). Feldman and Markiewicz argued in essence that the phase separation should cease to occur when kT becomes equal to the energy gained (at $T=0$) per pair by the phase separation. This is incorrect for a degenerate Fermi system. In fact, *free*-energy differences should be considered in deciding which configuration of the EHD is more stable at finite temperatures. But at low temperatures the free energy differs from the energy at $T=0$ by an amount proportional to T^2 which is smaller than kT, so that the effect of temperature on the EHD is much weaker than was supposed by Feldman and Markiewicz.